NeuroImage: Clinical 11 (2016) 743–750

Contents lists available at ScienceDirect

NeuroImage: Clinical

journal homepage: www.elsevier.com/locate/ynicl

Quantifying visual pathway axonal and myelin loss in multiple sclerosis and neuromyelitis optica

Praveena Manogaran[a], Irene M. Vavasour[b], Alex P. Lange[c], Yinshan Zhao[a], Katrina McMullen[a], Alexander Rauscher[d], Robert Carruthers[a], David K.B. Li[b], Anthony L. Traboulsee[a], Shannon H. Kolind[a,*]

[a]Department of Medicine, University of British Columbia, Vancouver, Canada
[b]Department of Radiology, University of British Columbia, Vancouver, Canada
[c]Department of Ophthalmology, University of British Columbia, Vancouver, Canada
[d]Department of Pediatrics, University of British Columbia, Vancouver, Canada

ARTICLE INFO

Article history:
Received 29 February 2016
Received in revised form 14 April 2016
Accepted 25 May 2016
Available online 26 May 2016

Keywords:
Multiple sclerosis
Neuromyelitis optica
Optical coherence tomography
Magnetic resonance imaging
Myelin water imaging
Optic neuritis

ABSTRACT

Background: The optic nerve is frequently injured in multiple sclerosis and neuromyelitis optica, resulting in visual dysfunction, which may be reflected by measures distant from the site of injury.
Objective: To determine how retinal nerve fiber layer as a measure of axonal health, and macular volume as a measure of neuronal health are related to changes in myelin water fraction in the optic radiations of multiple sclerosis and neuromyelitis optica participants with and without optic neuritis and compared to healthy controls.
Methods: 12 healthy controls, 42 multiple sclerosis (16 with optic neuritis), and 10 neuromyelitis optica participants (8 with optic neuritis) were included in this study. Optical coherence tomography assessment involved measurements of the segmented macular layers (total macular, ganglion cell layer, inner plexiform layer, and inner nuclear layer volume) and paripapillary retinal nerve fiber layer thickness. The MRI protocol included a 32-echo T_2-relaxation GRASE sequence. Average myelin water fraction values were calculated within the optic radiations as a measure of myelin density.
Results: Multiple sclerosis and neuromyelitis optica eyes with optic neuritis history had lower retinal nerve fiber layer thickness, total macular, ganglion cell and inner plexiform layer volumes compared to eyes without optic neuritis history and controls. Inner nuclear layer volume increased in multiple sclerosis with optic neuritis history (mean = 0.99 mm^3, SD = 0.06) compared to those without (mean = 0.97 mm^3, SD = 0.06; $p = 0.003$). Mean myelin water fraction in the optic radiations was significantly lower in demyelinating diseases (neuromyelitis optica: mean = 0.098, SD = 0.01, multiple sclerosis with optic neuritis history: mean = 0.096, SD = 0.01, multiple sclerosis without optic neuritis history: mean = 0.098, SD = 0.02; $F_{3,55} = 3.35$, $p = 0.03$) compared to controls. Positive correlations between MRI and optical coherence tomography measures were also apparent (retinal nerve fiber layer thickness and ganglion cell layer thickness: $r = 0.25$, $p = 0.05$, total macular volume and inner plexiform layer volume: $r = 0.27$, $p = 0.04$).
Conclusions: The relationship between reductions in OCT measures of neuro-axonal health in the anterior visual pathway and MRI-based measures of myelin health in the posterior visual pathway suggests that these measures may be linked through bidirectional axonal degeneration.

1. Introduction

Multiple sclerosis (MS) is characterized by demyelination and axonal damage in the central nervous system. Neuromyelitis optica (NMO) is an autoimmune disorder of the central nervous system that is characterized by episodes of inflammation and damage to astrocytes (Jacob et al., 2013). While MS and NMO have overlapping clinical features, treatment and prognosis differ significantly, consequently, misdiagnosis can result in worsening of symptoms and progression (Love, 2006). The recent discovery of an antibody (NMO-IgG) in the blood of individuals with NMO, facilitated differentiation of these two diseases, however, a correct diagnosis remains challenging, in particular, for those individuals with NMO who test negative for the antibodies (Jacob et al., 2013). The optic nerve is affected by inflammation (optic neuritis, ON) and lesions in both MS and NMO, resulting in considerable

* Corresponding author at: Department of Medicine, University of British Columbia, S-199 UBC Hospital, 2211 Wesbrook Mall, Vancouver, BC V6T2B5, Canada
E-mail addresses: p.manogaran@alumni.ubc.ca (P. Manogaran), lees@ubc.ca (I.M. Vavasour), alex@lange.ch (A.P. Lange), yinshan@mail.ubc.ca (Y. Zhao), katrina.mcmullen@ubc.ca (K. McMullen), rauscher@phas.ubc.ca (A. Rauscher), robert.carruthers@ubc.ca (R. Carruthers), david.li@ubc.ca (D.K.B. Li), t.traboulsee@ubc.ca (A.L. Traboulsee), shannon.kolind@ubc.ca (S.H. Kolind).

http://dx.doi.org/10.1016/j.nicl.2016.05.014

disability (Toosy et al., 2014). Clinical recovery from ON is often good, but subclinical abnormalities indicate incomplete recovery (Balcer et al., 2015). As a consequence of focal injury, retrograde and anterograde degeneration may affect the axons away from the lesion site (Kanamori et al., 2012; Siffrin et al., 2010). Retrograde degeneration due to ON can result in damage of the retinal nerve fiber layer and the macula which can be captured with optical coherence tomography (OCT), whereas damage to the optic radiation, a collection of myelinated axons carrying visual information to the cortex and a frequent site of injury in neurological disorders, can be assessed with MRI (Reich et al., 2009). While earlier work suggested differences in OCT measures between NMO and MS (Burkholder et al., 2009; Grazioli et al., 2008; Lange et al., 2013; Ratchford et al., 2009), a more comprehensive assessment of the visual pathway has not yet been performed. Comparison between retinal nerve fiber layer thickness, total macular volume, the individual retinal layers and myelination of the optic radiations may provide an opportunity to study how damage to one part of the visual pathway affects the other part. The aim of our study is to examine the segmented macular layers and to characterize the visual pathway in these two diseases using OCT neuro-axonal measures of the retina and a new MRI technique for the quantification of myelin loss in the brain.

2. Materials and methods

Twelve healthy controls, 42 remitting-relapsing MS participants (16 with ON, 26 without ON) and 10 NMO participants (8 with ON, 2 without ON) were included in this study. Subjects who met the recent Wingerchuk criteria (Wingerchuk et al., 2015) for an NMO spectrum disorder were included, regardless of whether they had been affected by a clinical episode of ON. Subjects who met the modified McDonald criteria (Polman et al., 2005) for clinically definite MS were also included. No participants were on steroid therapy at least one month prior to entering the study. ON history was characterized as having one or more episodes of ON in one or both eyes previous to entering the study. The healthy controls in this study had no history or signs of neurological diseases. Clinical characteristics of the participants such as high contrast visual acuity, disease duration, expanded disability status scale, and ON history were obtained through chart reviews. The University of British Columbia Clinical Research Ethics Board approved all study procedures and all subjects provided signed, informed consent before participating.

2.1. OCT protocol and analysis

The OCT assessment was conducted on a Heidelberg Spectralis Spectral-Domain OCT device (Software version 6.3.2.0; Heidelberg Engineering, Heidelberg, Germany). An online tracking system was used to compensate for eye movements.

The peripapillary retinal nerve fiber layer thickness protocol was done in high-resolution mode (axial resolution of 3.8 μm at 19,000 scans per second). 16 consecutive circular B-scans (each composed of 1536 A-scans) with a diameter of 3.4 mm were automatically averaged to reduce speckle noise (Lange et al., 2013). Several scans were taken by experienced operators and the best centered scans with a quality of at least 25 were chosen for analysis. The software calculated the objective refraction (spherical equivalent) and the overall mean retinal nerve fiber layer thickness was obtained.

The macular volume protocol involved 61 consecutive B-scans (ART 9; 768 A-scans each) horizontally crossing the macula for individuals with NMO and healthy controls. For individuals with MS, the macular volume was obtained using a built-in macular volume protocol ("PPoleN") consisting of 61 consecutive B-scans (ART 15; 768 A-scans each) vertically crossing the macula.

The macular data was automatically segmented using the Ganglion Cell Analysis Algorithm included in the Viewer Module (v.6.3.2.0). The software calculated the macular volume for the full retina (total macular volume), ganglion cell layer, inner plexiform layer, and inner nuclear layer (Fig. 1). All the images from automated segmentation were carefully reviewed by a trained examiner (P.M.) in a blind fashion.

2.2. MRI protocol and analysis

MRI scans were performed on a Philips 3.0T Achieva scanner (Best, the Netherlands) equipped with an 8-channel SENSE head coil. A 3D T_1-weighted spoiled gradient echo scan with repetition time of 6.5 ms, echo time of 3.6 ms, flip angle of 13° and 1.7 mm × 1.7 mm × 1.7 mm voxel size was acquired for segmentation of the tract of interest. An axial combined gradient echo and spin echo (GRASE) T_2 relaxation with 32 echoes sequence, repetition time of 1000 ms, echo time of 10–320 ms, echo spacing of 10 ms, 1 mm × 1 mm × 5 mm voxel size reconstructed to 1 mm × 1 mm × 2.5 mm, sensitivity encoding factor of 2 and an echo planar imaging factor of 3 was acquired for myelin water fraction estimation (Prasloski et al., 2012a). The scanned volume consisted of a 10 cm slab measured from the top of the brain caudally.

The signal decay curve obtained from the T_2 relaxation sequence was modelled by multiple exponential components and the T_2 distribution was estimated using non-negative least squares with the extended phase graph algorithm (Whittall & MacKay, 1969; Prasloski et al., 2012b). Myelin water fraction in each image voxel was computed as the ratio of the area under the T_2 distribution with times from 10–40 ms to the total area under the distribution (Laule et al., 2006). This analysis was performed using in-house software on Matlab® 2012 (MathWorks, Natick, Massachusetts, U.S.A).

For lesion identification, T2-weighted and proton density weighted scans were obtained. The T2-weighted and proton density weighted scans were acquired with a dual-echo sequence using repetition time of 2800 ms, first echo time of 8.42 ms, and second echo time of 80 ms for the NMO participants. All images for the NMO participants had dimensions of 256 × 256 × 60 and voxel size of 0.937 mm × 0.937 mm × 3.9 mm, with no inter-slice gap. For the MS participants, the T2-weighted images were acquired with a turbo-spin echo sequence using repetition time of 6100 ms, echo time of 80 ms, and turbo spin echo factor of 8. The proton density weighted images were acquired with a turbo-spin echo sequence using repetition time of 2000 ms, echo time of 10 ms, and turbo spin echo factor of 3. All images for the MS participants had dimensions of 256 × 256 × 60 and voxel size of 0.98 mm × 0.98 mm × 3 mm, with no inter-slice gap.

For the lesion masks, manual identification of the T2-weighted lesions was done with the placement of seed points and the rest of the processing is fully automatic (Tam et al., 2011; McAusland et al., 2010). After brain extraction (Smith, 2002), an experienced MRI radiologist was asked to place one or more seed points to mark the location and approximate extent of each lesion visible on the T2-weighted and proton density weighted scans.

The first echo image from the T_2 relaxation sequence was linearly co-registered to the anatomical 3D T_1 image using FMRIB's Linear Image Registration Tool (FLIRT) (Smith et al., 2004) to align the myelin water fraction results with the anatomical images for each individual. The calculated transformation matrix was then applied to the individual's myelin water fraction map. 3D T_1 images were co-registered to standard space using a combination of FLIRT and FNIRT (Andersson et al., 2007). Each individual's inverse transformation matrix for the registration between 3D T_1 and standard space was applied to the region of the optic radiation obtained from the Juelich Histological atlas (threshold 25%) to align the region with the 3D T_1 image (Fig. 2). The lesion masks were multiplied by the optic radiation mask to acquire the lesion load for only the optic radiations. Lesion volume was calculated by multiplying the image resolution (1.7 mm × 1.7 mm × 1.7 mm) with the lesion load obtained specifically for the optic radiations. This new mask was then manually edited to ensure only white matter was included and overlaid on the registered myelin water fraction images to obtain the mean myelin water fraction.

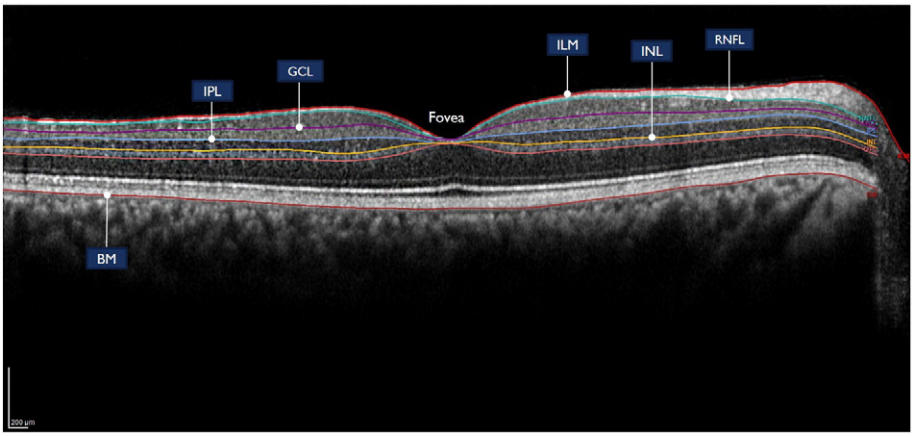

Fig. 1. Image of optical coherence tomography automated segmentation of the macular layers in a healthy control subject. Total macular volume is calculated between the ILM (inner limiting membrane) and BM (Bruch's membrane). Ganglion cell layer (GCL) is the volume between retinal nerve fiber layer (RNFL) and GCL. Inner plexiform layer (IPL) is the volume between GCL and IPL. Inner nuclear layer (INL) is calculated as the volume between IPL and INL.

2.3. Statistical analysis

2.3.1. Independent MRI and OCT analysis

Statistical analysis was performed using R: a language and environment for statistical computing (R Core Team, 2013; http://www.r-project.org). OCT and MRI measures were analyzed independently to identify differences between the study groups. A Shapiro-Wilk normality test determined that the data was normally distributed for all measures. For the analyses of peripapillary retinal nerve fiber layer thickness, macular ganglion cell layer, inner plexiform layer, inner nuclear layer volume and total macular volume, a linear mixed-effects model was used to account for intra-patient inter-eye dependencies, with group, age, gender and ON history included as covariates. Based on this model, we assessed the differences between study groups as well as between eyes with and without ON history. For the optic radiation myelin water fraction, initial analysis showed no significant ON history, age or gender effect and therefore a linear regression model was not used to account for these factors. Instead, a one-way analysis of variance (ANOVA) was performed to compare the four groups: healthy controls, MS with ON history and those without ON history, and NMO subjects. The NMO group only had two subjects without ON history so they were not subdivided (preliminary analysis showed no clear difference when subdivided). Post-hoc analysis employed Fisher's LSD test to compare all pairs of the four study groups. P-values equal to or below 0.05 were taken to be significant. No adjustments were made to the p-values due to the exploratory nature of this study.

2.3.2. Correlation analysis

The relationship between the individual OCT measures and the optic radiation myelin water fraction were assessed using a Pearson product-moment correlation. The relationship between the lesion volume in the optic radiation with the retinal nerve fiber layer thickness and ganglion cell layer volume was assessed using a Spearman's ranked correlation in MS and NMO participants with and without optic neuritis. For the analysis in this section, the minimum retinal nerve fiber layer thickness and macular volume values between the two eyes of each individual was used because the optic radiation tracts from both hemispheres are associated with each eye and the myelin water imaging resolution is not high enough to separate out contributions from the left and right eye. The correlations were not adjusted for multiple comparisons. P-values equal to or below 0.05 were taken to be significant.

3. Results

The clinical characteristics for all participants are shown in Table 1. All but three subjects in the NMO group were NMO-IgG positive. Two subjects in the NMO group and 26 subjects in the MS group did not have a clinical episode of ON. One participant with MS was on treatment (minocycline) at the time of testing. Four participants with NMO were on mycophenolic acid (CellCept®), three on azathioprine (Imuran®), and one participant each on either interferon beta-1a (Rebif 44®), mitoxantrone or rituximab. There were five cases of bilateral ON in the MS and also in the NMO study groups. One among 12 healthy volunteers was excluded from OCT analysis because of epiretinal membrane discovered during examination of the macular segmentation. The right eye of two MS subjects, one healthy volunteer and the left eye of one NMO subject were excluded from the macular volume analysis due to poor quality. One individual with NMO did not have the OCT measures for the left eye due to poor vision making it difficult to fixate but their right eye was still included in all of the analysis. Four individuals with MS did not have an MRI performed due to scheduling issues, claustrophobia and other MRI contraindications.

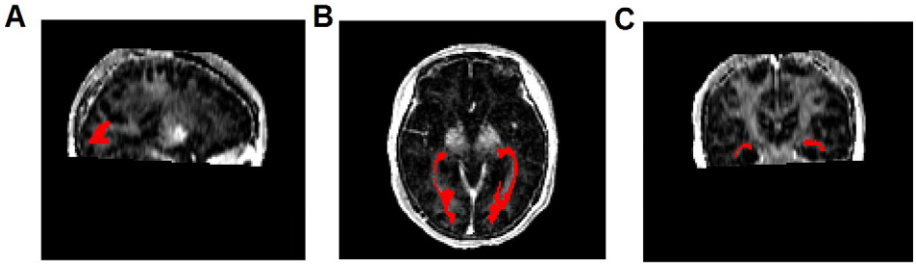

Fig. 2. The optic radiation region of interest (in red) obtained using myelin water imaging from an individual with neuromyelitis optica. (A) sagittal view (B) axial view (C) coronal view.

Table 1
Subject characteristics and results. The mean of each measure is presented except for sex (ratio of male to female) and EDSS (median). Standard deviation is in parentheses except for EDSS (range).

Technique	Measurement	Control	MS	MS-NON	MS-ON	NMO	NMO-NON	NMO-ON
Clinical	# of subjects	12	42	26	16	10	2	8
	Age (years)	31.2 (9.6)	39.5 (9.6)	40.3 (9.6)	38.3 (9.7)	43.2 (11.2)	39.0 (3.0)	47.9 (13.0)
	Sex (M:F)	3:9	17:25	10:16	7:9	3:7	1:1	2:6
	EDSS	–	2.0 (0–4)	1.75 (0–4)	2.0 (0–4)	2.5 (2.0-6.0)	2.5 (2.5–2.5)	2.5 (2.0–6.0)
	Disease duration (years)	–	6.8 (5.4)	5.8 (4.6)	8.8 (6.5)	6.0 (3.9)	7.0 (0)	5.8 (4.3)
	VA OD (logMAR)	–	0.1 (0.1)	0.1 (0.1)	0.1 (0.1)	0.0 (0.1)	0.0 (0)	0.0 (0.1)
	VA OS (logMAR)	–	0.1 (0.2)	0.1 (0.1)	0.1 (0.2)	0.2 (0.4)	0.0 (0)	0.3 (0.4)
	Last ON attack (years)	–	–	–	4.2 (4)	–	–	4.7 (3)
OCT	RNFL thickness (μm)	100.1 (10.8)	90.4 (12.7)	93.5 (11.1)	81.0 (12.8)	76.0 (19.1)	87.3 (20.9)	70.8 (16.4)
	TMV (mm^3)	8.73 (0.3)	8.47 (0.4)	8.58 (0.4)	8.14 (0.3)	8.13 (0.4)	8.34 (0.5)	8.03 (0.3)
	GCL volume (mm^3)	1.09 (0.06)	1.00 (0.1)	1.03 (0.1)	0.89 (0.08)	0.89 (0.1)	0.96 (0.1)	0.86 (0.1)
	IPL volume (mm^3)	0.90 (0.04)	0.84 (0.08)	0.86 (0.07)	0.76 (0.06)	0.77 (0.09)	0.82 (0.09)	0.74 (0.08)
	INL volume (mm^3)	0.96 (0.04)	0.97 (0.06)	0.97 (0.06)	0.99 (0.06)	0.94 (0.06)	0.97 (0.04)	0.92(0.06)
MRI	OR MWF	0.113 (0.01)	0.0969 (0.01)	0.0975 (0.02)	0.0961 (0.01)	0.0977 (0.01)	0.101 (0.009)	0.0969 (0.01)
	Lesion volume (mm^3)	–	251.6 (267)	201.4 (227)	316.2 (308)	35.1 (50)	22.1 (31)	33.6 (55)

MS: multiple sclerosis; NMO: neuromyelitis optica; EDSS: expanded disability status scale; VA: visual acuity; OD: right eye; OD: left eye; ON: optic neuritis; Last ON attack: time between last ON attack and entry into study; RNFL: retinal nerve fiber layer; TMV: total macular volume; GCL: ganglion cell layer; IPL: inner plexiform layer; INL: inner nuclear layer; OR: optic radiations; MWF: myelin water fraction.
MS: All MS eyes (for OCT) or all individuals with MS (for MRI and Clinical);
MS-NON: MS eyes without ON history (for OCT) or MS patients without ON history (for MRI and Clinical);
MS-ON: MS eyes with ON history (for OCT) or MS patients with ON history (for MRI and Clinical);
NMO: All NMO eyes (for OCT) or all individuals with NMO (for MRI and Clinical);
NMO-NON: NMO eyes without ON history (for OCT) or NMO patients without ON history (for MRI and Clinical);
NMO-ON: NMO eyes with ON history (for OCT) or NMO patients with ON history (for MRI and Clinical).

3.1. OCT assessment

3.1.1. Retinal nerve fiber layer thickness

In total, there were 21 MS eyes with ON (MS-ON), 63 MS eyes without ON (MS-NON), 13 NMO eyes with ON (NMO-ON), 6 NMO eyes without ON history (NMO-NON), and 22 healthy control eyes. There was a decrease in peripapillary retinal nerve fiber layer thickness in MS-ON (mean = 81.0 μm, SD = 12.8) compared to healthy control eyes (mean = 100.1 μm, SD = 10.8; p = 0.005; Fig. 3A). Retinal nerve fiber layer thickness was lower in NMO-ON (mean = 70.8 μm, SD = 16.4) compared to healthy controls eyes (p = 0.00001; Fig. 3A). Both MS-ON and NMO-ON had lower retinal nerve fiber layer thickness

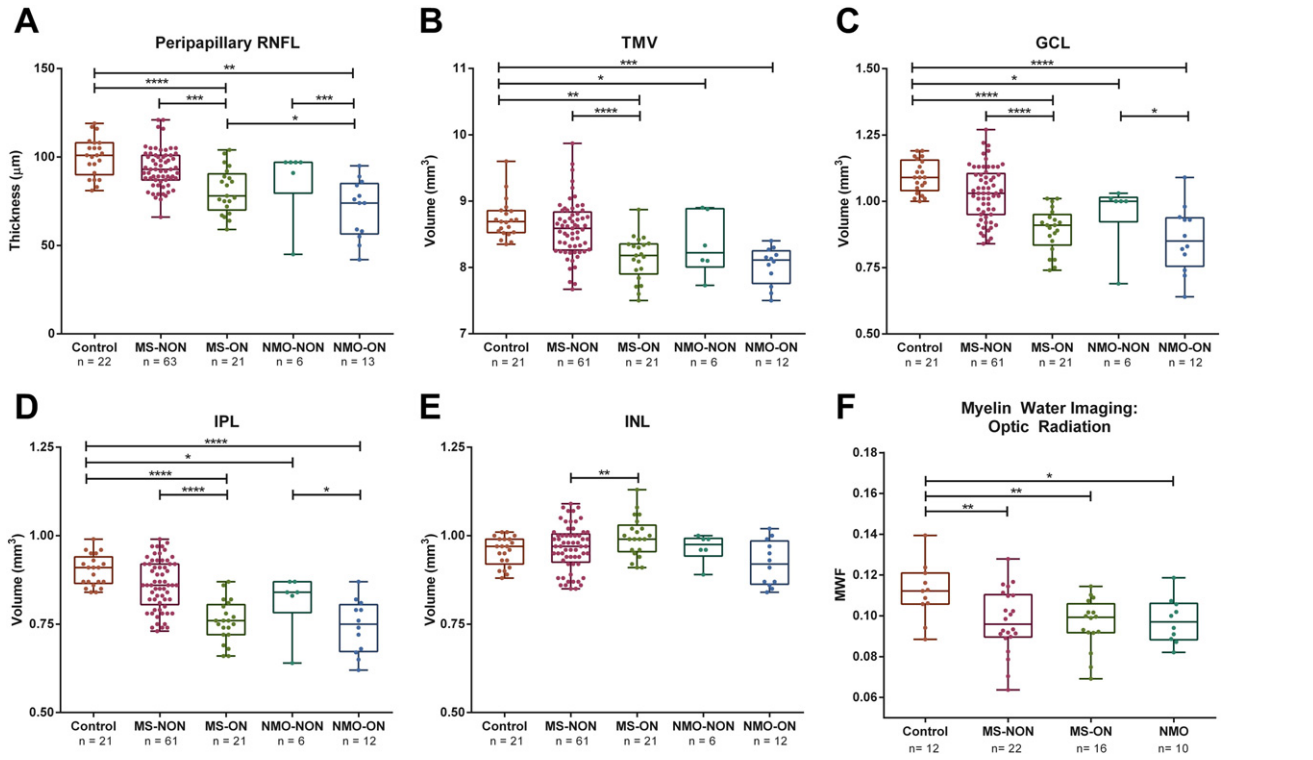

Fig. 3. Boxplots of the (A) peripapillary RNFL thickness, (B) TMV, (C) GCL volume, (D) IPL volume, (E) INL volume, and (F) myelin water imaging of the optic radiations in healthy controls, individuals with neuromyelitis optica and multiple sclerosis. The p-values were based on a linear mixed-effects model accounting for intra-patient inter-eye dependencies, age, gender and ON history. *$p < 0.05$, **$p \le 0.01$, ***$p \le 0.001$, ****$p \le 0.0001$. n is the number of eyes for each group. RNFL: retinal nerve fiber layer, TMV: total macular volume, GCL: ganglion cell layer, IPL: inner plexiform layer; INL: inner nuclear layer, Control: healthy control subjects, ON: optic neuritis, NMO-ON: neuromyelitis optica with ON history, NMO-NON: neuromyelitis optica without ON history, MS-ON: multiple sclerosis with ON history, MS-NON: multiple sclerosis without ON history.

than those without ON (MS-NON: mean = 93.5 μm, SD = 11.1; NMO-NON: mean = 87.3 μm, SD = 20.9; p = 0.0001 and p = 0.0008 respectively; Fig. 3A). NMO-ON had significant retinal nerve fiber layer thinning compared to MS-ON (p = 0.02, Fig. 3A).

3.1.2. Total macular volume

For all following macular assessments there were 21 MS-ON, 61 MS-NON, 12 NMO-ON, 6 NMO-NON, and 21 healthy control eyes included. Similar to retinal nerve fiber layer thickness results, total macular volume was lower in NMO-ON (mean = 8.03 mm^3, SD = 0.3), NMO-NON (mean = 8.34 mm^3, SD = 0.5), and MS-ON (mean = 8.14 mm^3, SD = 0.3) compared to healthy control eyes (mean = 8.73 mm^3, SD = 0.3; p = 0.0006, p = 0.03 and p = 0.002 respectively; Fig. 3B). For MS-ON, total macular volume was lower compared to eyes without (MS-NON: mean = 8.58 mm^3, SD = 0.4, p = 0.000005; Fig. 34B). Unlike with retinal nerve fiber layer thickness, NMO-ON did not differ significantly compared to eyes without (p = 0.2; Fig. 3B).

3.1.3. Ganglion cell layer volume

Ganglion cell layer volume was significant lower in NMO-ON (mean = 0.86 mm^3, SD = 0.1), NMO-NON (mean = 0.96 mm^3, SD = 0.1), MS-ON (mean = 0.89 mm^3, SD = 0.08) compared to healthy controls (mean = 1.09 mm^3, SD = 0.06; p = 0.0000004, p = 0.02, and p = 0.000001 respectively; Fig. 3C). The MS-ON group had significantly lower volume in the ganglion cell layer compared to MS-NON (MS-NON: mean = 1.03 mm^3, SD = 0.1; p = 0.0000003) and this difference was also seen between the NMO-ON and NMO-NON groups (p = 0.05; Fig. 3C).

3.1.4. Inner plexiform layer volume

Inner plexiform layer volume was significant lower in NMO-ON (mean = 0.74 mm^3, SD = 0.08), NMO-NON (mean = 0.82 mm^3, SD = 0.09), MS-ON (mean = 0.76 mm^3, SD = 0.06) compared to healthy controls (mean = 0.90 mm^3, SD = 0.04; p = 0.0000007, p = 0.02, and p = 0.000003 respectively; Fig. 3D). MS eyes with ON history had significantly lower volume in the inner plexiform layer compared to eyes without ON history (MS-NON: mean = 0.86 mm^3, SD = 0.07; p = 0.000000006) and NMO eyes with ON history also had lower inner nuclear layer volume compared to eyes without (p = 0.03; Fig. 3D).

3.1.5. Inner nuclear layer volume

The inner nuclear layer volume was significantly higher in MS-ON (mean = 0.99 mm^3, SD = 0.06) compared to MS-NON (mean = 0.97 mm^3, SD = 0.06; p = 0.003; Fig. 3E). There were no statistically significant difference between MS-NON, MS-ON, NMO-NON (mean = 0.97 mm^3, SD = 0.04), or NMO-ON (mean = 0.92 mm^3, SD = 0.06) eyes compared to healthy controls (mean = 0.96 mm^3, SD = 0.04; p = 0.5, p = 0.1, p = 0.4, and p = 0.8 respectively; Fig. 3E). Inner nuclear layer volume also did not differ between NMO-NON and NMO-ON (p = 0.3; Fig. 3E).

3.2. MRI assessment

Myelin water fraction measures of the optic radiations were different between the four groups ($F_{3,56}$ = 4.15, p = 0.01; Fig. 3F). The NMO group (mean = 0.098, SD = 0.01, n = 10), the MS-ON (mean = 0.096, SD = 0.01, n = 16) and the MS-NON group (mean = 0.098, SD = 0.02, n = 26) had lower optic radiation myelin water fraction when compared to healthy controls (mean = 0.113, SD = 0.01, n = 12; t_{56} = 2.54, p = 0.01; t_{56} = 3.15, p = 0.003; and t_{56} = 3.07, p = 0.003 respectively; Fig. 3F). The myelin water fraction did not differ between the MS-ON and NMO cohort (t_{56} = 0.28, p = 0.8), MS-NON and NMO cohort (t_{56} = 0.035, p = 1.0) or between MS-ON and MS-NON cohort (t_{56} = 0.31, p = 0.8; Fig. 3F).

3.3. Correlation analysis

A significant positive correlation was observed between optic radiation myelin water fraction and retinal nerve fiber layer thickness (r(59) = 0.25, p = 0.05; Fig. 4A). There was also a significant positive correlation between optic radiation myelin water fraction and total macular volume (r(59) = 0.27, p = 0.04; Fig. 4B), ganglion cell layer volume (r(59) = 0.25, p = 0.05; Fig. 4C), or inner plexiform layer volume (r(59) = 0.27, p = 0.04; Fig. 4D). There was no statistically significant correlation between inner nuclear layer volume and optic radiation myelin water fraction (r(59) = 0.06, p = 0.6). No statistically significant correlation was observed between lesion volume of the optic radiations and retinal nerve fiber layer thickness (r(39) = −0.1, p = 0.4) or ganglion cell layer volume (r(39) = −0.03, p = −0.9).

4. Discussion

This study assessed the anterior and posterior visual pathways in individuals with MS, NMO and healthy controls using OCT and MRI measurements and looked at the relationship between these parameters. No studies to date have assessed the relationship between the specific segmented retinal layers using OCT and MRI measures in NMO. Additionally, this is the first study to use myelin water imaging to quantify myelin content in the optic radiations of demyelinating diseases.

Similar to previous findings (Burkholder et al., 2009; Ratchford et al., 2009; Frohman et al., 2008; Siger et al., 2008), retinal nerve fiber layer thinning and decreased total macular volume was most pronounced in NMO eyes with ON history followed by MS eyes with ON history compared to unaffected eyes in MS and NMO and healthy control eyes. This finding is consistent with the concept of retrograde degeneration in the retina, secondary to ON. Retinal nerve fiber layer thickness was thinner in NMO eyes with ON history compared to MS eyes with ON history, providing support for the notion that ON attacks are usually more severe with incomplete recovery in NMO than MS. Retrograde loss of retinal ganglion cells has been observed in primate studies when the optic nerve was transected (Quigley et al., 1977). It is also possible that retrograde degeneration to the macula is occurring secondary to retinal nerve fiber layer axonal loss (Trip et al., 2005). The lack of difference in the total macular volume measure between NMO eyes with ON history and eyes without is likely due to the small sample size of the NMO group, as previous research did find a significant difference between these groups (Smith, 2002; Schneider et al., 2013).

Retinal nerve fiber layer and macular volume loss in non-ON MS eyes may be due to lesions within the posterior optic pathway that could result in retrograde degeneration to the retina (Petzold et al., 2010; Noval et al., 2011). Another possibility is the presence of clinically silent demyelinating lesions within the optic nerve that result in retrograde degeneration to the retinal nerve fiber layer/macula in unaffected MS eyes (Henderson et al., 2008), however lesions were not looked for in this study.

The ganglion cell layer volume decrease in demyelinating diseases compared to healthy controls is likely due to retrograde degeneration of retinal nerve fiber layer axons towards their associated ganglion cell bodies which is also worse in eyes with ON history than those without (Walter et al., 2012; Zimmermann et al., 2012). Results were similar in the inner plexiform layer which is likely due to the damage propagating from the retinal ganglion cells to the dendrites located there.

Interestingly, there was a decrease in the total macular volume, ganglion cell layer and inner plexiform layer volume in NMO eyes without ON history compared to controls. The decreased volume might be due to subclinical disease activity, commonly recognized in MS but only recently explored in NMO (Schneider et al., 2013; Walter et al., 2012; Syc et al., 2012). One speculation is that damage in these layers might result from anti-AQP4 mediated pathology to Müller cells that span the thickness of the retina and highly express AQP4 channels (Syc et al., 2012).

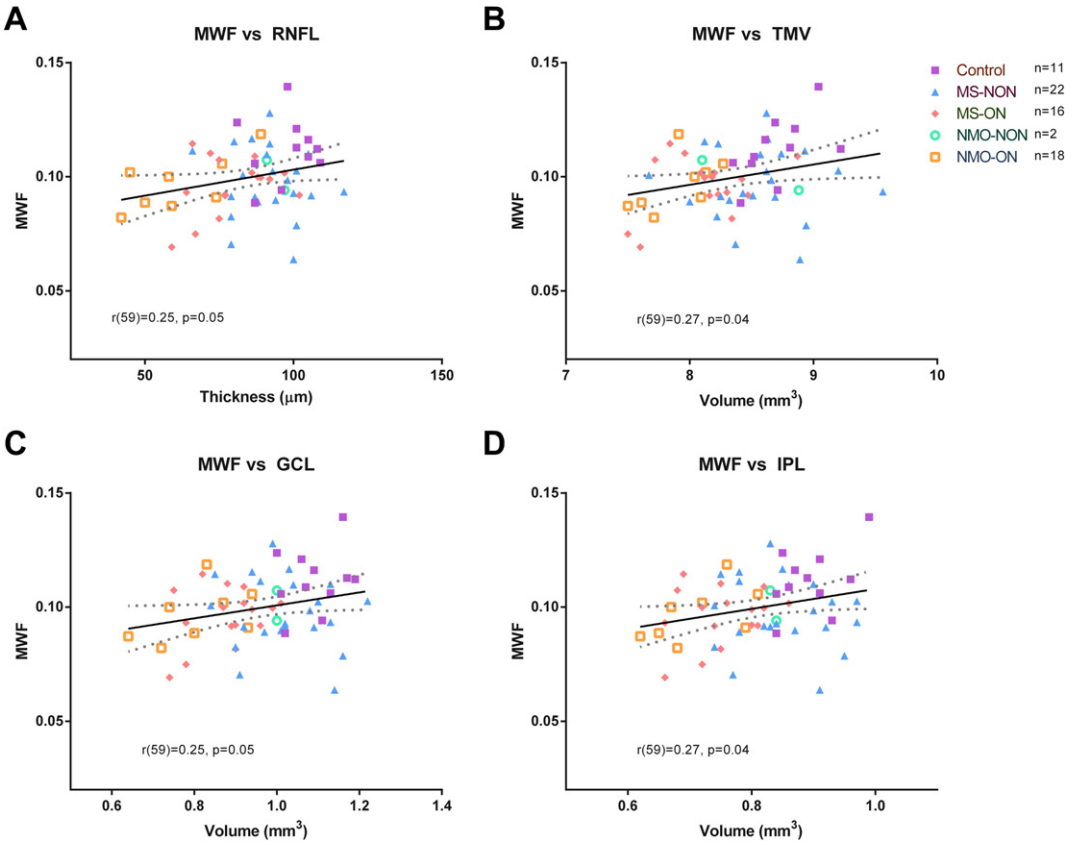

Fig. 4. The relationship between OCT and MRI measures in all subjects. (A) Positive correlation between MWF in the optic radiations and RNFL thickness, (B) a positive correlation between MWF in the optic radiations and the TMV, (C) a positive correlation between MWF in the optic radiations and GCL, and (D) a positive correlation between MWF in the optic radiations and IPL volume. Minimum RNFL thickness and macular volumes between the two eyes were used for comparisons with MWF in the optic radiations. 95% confidence interval is shown in dotted line. n is the number of subjects in each group. OCT: optical coherence tomography, MRI: magnetic resonance imaging, MWF: myelin water fraction, NMO: neuromyelitis optica, MS: multiple sclerosis, ON: optic neuritis, NMO-ON: NMO with ON history, NMO-NON: NMO without ON history, MS-ON: MS with ON history, MS-NON: MS without ON history, CON: healthy control, RNFL: retinal nerve fiber layer, TMV: total macular volume, GCL: ganglion cell layer, IPL: inner plexiform layer, INL: inner nuclear layer.

There was a significant increase in the inner nuclear layer volume of MS subjects with ON history compared to those without. The inner nuclear layer is primarily composed of bipolar cells and also contains horizontal, amacrine and Müller cell bodies (Fernandes et al., 2013). Our population of MS and NMO patients did not have microcystic macular edema which has been linked to Müller cell pathology and generally thought to be related to inner nuclear layer volume increase (Schneider et al., 2013; Gelfand et al., 2013). This provides further support suggesting that inner nuclear layer thickening in MS patients with ON history may occur independently of microcystic macular edema, as previously observed (Gabilondo et al., 2015). The lack of damage in the inner nuclear layer of the NMO eyes with ON history might suggest that retrograde degeneration does not necessarily extend to the deeper layers of the retina (Syc et al., 2012).

The observed decrease in myelin water fraction in MS subjects with ON history and NMO subjects (predominantly affected by ON) compared to healthy controls may be due to anterograde degeneration from damage to the optic nerve (Green et al., 2010). Decreased myelin water fraction suggests reduced myelin density in the optic radiations of these subjects (Laule et al., 2006). Re-analysis of the optic radiation myelin water fraction without the inclusion of lesions did not change the above results. In addition to anterograde degeneration, MS optic radiations could be affected by lesions that typically accumulate in the periventricular and subcortical white matter that involves optic radiations tracts (Reich et al., 2009).

The decrease in myelin water fraction in the MS subjects without ON history compared to controls suggests that the underlying disease in MS may cause damage to the visual pathway in the absence of ON (Reich et al., 2009). There may be a greater presence of subclinical optic nerve damage in MS with axonal attrition independent of ON attacks or due to an increased probability of MS lesions appearing in the optic chiasm and tract (Noval et al., 2011; Pfueller & Paul, 2011). The general neurodegeneration and ongoing progressive neuro-axonal loss in MS brain and retina may be compounded by the additional axonal loss due to ON which aren't directly linked (Zimmermann et al., 2012; Noval et al., 2011). However, unlike MS, NMO predominantly involves a series of relapses and rarely presents with secondary progression or diffuse low grade inflammation throughout normal appearing central nervous system tissue (Grazioli et al., 2008; Gelfand et al., 2013). Yu and colleagues observed abnormal diffusion in the brain white matter of NMO patients restricted to regions with connections to the spinal cord and optic nerve suggesting that the abnormal diffusion is likely due to damage in those regions (Yu et al., 2008).

Histopathological studies have shown that the myelin water fraction qualitatively corresponds to the anatomic distribution of myelin (Laule et al., 2006; Laule et al., 2008; Kozlowski et al., 2008). Myelin water imaging may provide a more specific measure of changes in myelin compared to other advancing imaging tools such as magnetization transfer imaging and diffusion tensor imaging (Alonso-Ortiz et al., 2015). A previous study using diffusion tensor imaging found that the optic radiations were significantly abnormal in MS subjects compared to controls and suggested an association between reduced retinal nerve fiber layer thickness and optic radiation damage similar to the results found in our study (Reich et al., 2009). However, unlike myelin water imaging, diffusion tensor imaging is non-specific and reflects not only myelin but also axonal density, membrane permeability and fiber coherence (Beaulieu, 2002; Harsan et al., 2006).

Optic radiation abnormalities have been observed in other neurological diseases. Optic radiation damage suggestive of Wallerian degeneration was identified in patients with lateral geniculate nucleus lesions (Reich et al., 2009). The loss of neurons in the lateral genicular nucleus of individuals with MS may also be due to anterograde trans-synaptic degeneration from optic nerve damage (Green et al., 2010). Diffuse abnormalities along the entire tract were observed in MS patients with ON history from the lateral geniculate nucleus, to the optic radiations and finally to the occipital cortex (Barkhof et al., 2009).

The association between retinal nerve fiber layer thinning, macular volume (total macular, ganglion cell layer and inner plexiform layer volume) and decreased myelin in the posterior visual pathway provides further support for how damage to one part of the visual pathway may cause, via antero- or retrograde degeneration, alterations in another part of the visual system. Previous studies have found similar correlations between MRI measures (such as brain parenchymal fraction, and magnetization transfer imaging) and retinal nerve fiber layer thickness and total macular volume in MS and patients with ON (Siger et al., 2008; Barkhof et al., 2009; Frohman et al., 2009; Ciccarelli et al., 2005). Additionally, when examining the segmented macular layers, other studies have found associations between ganglion cell layer and inner plexiform layer and whole brain volume (Saidha et al., 2015) or between ganglion cell layer and white/grey matter volume (Zimmermann et al., 2012; Balk et al., 2015) or lesions in optic radiations in MS. Lesion volume in the optic radiations did not correlate with OCT measures contrary to previously reported studies (Reich et al., 2009; Gabilondo et al., 2014). The lack of correlation may be due to the sample size, as not all subjects had brain lesions. It may also suggest that damage in the anterior visual pathway isn't related to lesions affecting the optic radiation fibers but may be due to subclinical disease mechanisms. However, this is only a correlation, therefore, future studies using animal models or post-mortem data is needed to explore reasons for the perceived relationship.

There are some limitations to this exploratory study. The sample size for the NMO and healthy control cohorts was small; however, a significant difference was still observed in the MRI and OCT measures between all the groups. OCT measurements of the macular volume and lesion identification were conducted under slightly different protocols in the MS and NMO group. This might have contributed to the differences in the OCT results between the two groups, however they were consistent with the retinal nerve fiber layer measures and previous studies. The MS and NMO participants were on a variety of different treatments. The effect of treatment on the visual pathway and myelin water imaging is currently unknown. Due to the small number of cases of NMO worldwide, there is a paucity of research in the field limiting the understanding of the pathogenesis of NMO. Future work should evaluate more specific relationships between brain structure-function changes, perhaps with visual function assessments such as visual evoked potential as well as additional visual tests and disease duration. This exploratory study suggests differences between MS and NMO in the visual system that warrants further investigation.

5. Conclusions

The relationship between reductions in OCT measures of neuronal and axonal health in the anterior visual pathway and MRI-based measures of myelin health in the posterior visual pathway suggests that these measures are likely linked through anterograde and retrograde axonal degeneration. Imaging techniques like OCT and myelin water imaging have not yet been used to their full potential, especially in studies focusing on the entire visual pathway. Using these imaging techniques to focus on the optical pathway can help identify important differences between MS and NMO and give further insight into NMO-specific damage processes as well as trans-synaptic damage processes independent of the underlying disease.

Conflict of interest statement

I.M. Vavasour has received research support from Genzyme Corporation and Hoffman La-Roche. A. Rauscher has received honoraria from Roche Pharmaceuticals (unrelated to MS). He is also supported by a Canadian Institutes for Health Research New Investigator Award. R. Carruthers has received personal compensation from Biogen, Teva and Genzyme for speaking. He is involved in clinical trials sponsored by Genzyme, Biogen, Novartis, Genzyme, Roche, Chugai including acting as site PI for trials sponsored by Teva and MedImmune. D.K. Li has received research funding from the Canadian Institute of Health Research and Multiple Sclerosis Society of Canada. He is the director of the UBC MS/MRI Research Group, which has been contracted to perform central analysis of MRI scans for therapeutic trials with Genzyme, Hoffmann-LaRoche, Merck-Serono, Nuron, Perceptives and Sanofi-Aventis. He has also acted as a consultant to Vertex Pharmaceuticals and served on the data and safety advisory boards for Novartis, Nuron and Roche. A.L. Traboulsee has received personal compensation from Chugai, Genzyme, Novartis, Roche, Serono and Teva Innovation for consulting. He has also received research support for principle investigator on clinical trials with Genzyme and Roche. S.H. Kolind has served on scientific advisory boards and received honoraria from Roche, Genzyme and EMD Serono for serving on a scientific advisory board. She has received research support from Roche for an advanced MRI study. A part of S.H. Kolind's salary was supported by Milan & Maureen Ilich Foundation. All other authors have no conflicts of interest to declare.

Acknowledgements

The UBC MRI Research Centre acknowledges the support of Philips Healthcare, F. Hoffmann-La Roche Ltd. and thanks its technologists. Thank you also to the UBC MS/MRI Reseach Group, MS clinical trials team and volunteers. The first author thanks Julia Schubert, William D. Regan, Chantal Roy-Hewitson, and Jacqueline Li for helping with recruitment and data collection. A part of this study was supported by funding by Bayer Pharmaceutical and funding support from Susan and Rick Diamond for NMO research. A part of S.H. Kolind's salary was supported by Milan & Maureen Ilich Foundation.

References

Alonso-Ortiz, E., Levesque, I.R., Pike, G.B., 2015. MRI-based myelin water imaging: a technical review. MRM 73, 70–81.
Andersson, J., Jenkinson, M., Smith, S., 2007. Non-linear optimization. Technical Report for FMRIB Analysis Group. Report no. TR07JA1, 28 June. FMRIB Centre, Oxford.
Balcer, L., Miller, D., Reingold, S., et al., 2015. Vision and vision-related outcome measures in multiple sclerosis. Brain 138, 11–27.
Balk, L.J., Steenwijk, M.D., Tewarie, P., et al., 2015. Bidirectional trans-synaptic axonal degeneration in the visual pathway in multiple sclerosis. J. Neurol. Neurosurg. Psychiatry 86 (4), 419–424.
Barkhof, F., Calabresi, P., Miller, D., et al., 2009. Imaging outcomes for neuroprotection and repair in multiple sclerosis trials. Nat. Rev. Neurol. 5 (5), 256–266.
Beaulieu, C., 2002. The basis of anisotropic water diffusion in the nervous system – a technical review. NMR Biomed. 15 (7–8), 435–455.
Burkholder, B., Osborne, B., Loguidice, M., et al., 2009. Macular volume determined by optical coherence tomography as a measure of neuronal loss in multiple sclerosis. Arch. Neurol. 66 (11), 1366–1372.
Ciccarelli, O., Toosy, A., Hickman, S., et al., 2005. Optic radiation changes after optic neuritis detected by tractography-based group mapping. Hum. Brain Mapp. 25 (3), 308–316.
Fernandes, D.B., Raza, A.S., Nogueira, R., et al., 2013. Evaluation of inner retinal layers in patients with multiple sclerosis or neuromyelitis optica using optical coherence tomography. Ophthalmology 120 (2), 387–394.
Frohman, E., Fujimoto, J., Frohman, T., et al., 2008. Optical coherence tomography: a window into the mechanisms of multiple sclerosis. Nat. Clin. Pract. Neurol. 4 (12), 664–675.
Frohman, E., Dwyer, M., Frohman, T., et al., 2009. Relationship of optic nerve and brain conventional and non-conventional MRI measures and retinal nerve fiber layer thickness, as assessed by OCT and GDx: a pilot study. J. Neurol. Sci. 282 (1), 96–105.
Gabilondo, I., Martinez-Lapiscina, E.H., Martinez-Heras, E., et al., 2014. Trans-synaptic axonal degeneration in the visual pathway in multiple sclerosis. Ann. Neurol. 75, 98–107.
Gabilondo, I., Martinez-Lapiscina, E.H., Fraga-Pumar, E., et al., 2015. Dynamics of retinal injury after acute optic neuritis. Ann. Neurol. 77, 517–528.

Gelfand, J.M., Cree, B.A., Nolan, R., et al., 2013. Microcystic inner nuclear layer abnormalities and neuromyelitis optica. JAMA Neurol 70 (3), 629–633.
Grazioli, E., Zivadinov, R., Weinstock-Guttman, B., et al., 2008. Retinal nerve fiber layer thickness is associated with brain MRI outcomes in multiple sclerosis. J. Neurol. Sci. 268 (1), 12–17.
Green, A., McQuaid, S., Hauser, S., et al., 2010. Ocular pathology in multiple sclerosis: retinal atrophy and inflammation irrespective of disease duration. Brain 133 (6), 1591–1601.
Harsan, L.A., Poulet, P., Guignard, B., et al., 2006. Brain dysmyelination and recovery assessment by noninvasive in vivo diffusion tensor magnetic resonance imaging. J. Neurosci. Res. 83 (3), 392–402.
Henderson, A., Trip, S., Schlottmann, P., et al., 2008. An investigation of the retinal nerve fibre layer in progressive multiple sclerosis using optical coherence tomography. Brain 131 (1), 277–287.
Jacob, A., McKeon, A., Nakashima, I., et al., 2013. Current concept of neuromyelitis optica (NMO) and NMO spectrum disorders. J. Neurol. Neurosurg. Psychiatry 84, 922–930.
Kanamori, A., Catrinescu, M., Belisle, J., et al., 2012. Retrograde and Wallerian axonal degeneration occur synchronously after retinal ganglion cell axotomy. Am. J. Pathol. 181 (1), 62–73.
Kozlowski, P., Liu, J., Yung, A.C., et al., 2008. High-resolution myelin water measurements in rat spinal cord. Magn. Reson. Med. 59 (4), 769–802.
Lange, A., Sadjadi, R., Zhu, F., et al., 2013. Spectral domain optical coherence tomography of retinal nerve fiber layer thickness in NMO patients. J. Neuroophthalmol. 33 (3), 213–219.
Laule, C., Leung, E., Lis, D., et al., 2006. Myelin water imaging in multiple sclerosis: quantitative correlations with histopathology. Mult. Scler. 12, 747–753.
Laule, C., Kozlowski, P., Leung, E., et al., 2008. Myelin water imaging of multiple sclerosis at 7 T: correlations with histopathology. NeuroImage 40 (4), 1575–1580.
Love, S., 2006. Demyelinating diseases. J. Clin. Pathol. 59 (11), 1151–1159.
McAusland, J., Tam, R.C., Wong, E., et al., 2010. Optimizing the use of radiologist seed points for improved multiple sclerosis lesion segmentation. Biomed. Eng. 57 (11), 2689–2698.
Noval, S., Contreras, I., Munoz, S., et al., 2011. Optical coherence tomography in multiple sclerosis and neuromyelitis optica: an update. Mult Scler Int, 472790.
Petzold, A., de Boer, J., Schippling, S., et al., 2010. Optical coherence tomography in multiple sclerosis: a systematic review and meta-analysis. Lancet Neurol. 9 (9), 921–932.
Pfueller, C., Paul, F., 2011. Imaging the visual pathway in neuromyelitis optica. Mult Scler Int, 869814.
Polman, C., Reingold, S., Edan, G., et al., 2005. Diagnostic criteria for multiple sclerosis: 2005 revisions to the "McDonald Criteria". Ann. Neurol. 58 (6), 840–846.
Prasloski, T., Rauscher, A., MacKay, A., et al., 2012a. Rapid whole cerebrum myelin water imaging using a 3D GRASE sequence. NeuroImage 63, 533–539.
Prasloski, T., Mädler, B., Xiang, Q.S., et al., 2012b. Applications of stimulated echo correction to multicomponent T2 analysis. Magn. Reson. Med. 67, 1803–1814.
Quigley, H., Davis, E., Anderson, D., 1977. Descending optic nerve degeneration in primates. Investig. Ophthalmol. Vis. Sci. 16 (9), 841–849.
Ratchford, J., Quigg, M., Conger, A., et al., 2009. Optical coherence tomography helps differentiate neuromyelitis optica and MS optic neuropathies. Neurology 73 (4), 302–308.
Reich, D., Smith, S., Gordon-Lipkin, E., et al., 2009. Damage to the optic radiation in multiple sclerosis is associated with retinal injury and visual disability. Arch. Neurol. 66 (8), 998–1006.
Saidha, S., Al-Louzi, O., Ratchford, J.N., et al., 2015. Optical coherence tomography reflects brain atrophy in multiple sclerosis: a four year study. Ann. Neurol. 78 (5), 801–813.
Schneider, E., Zimmermann, H., Oberwahrenbrock, T., et al., 2013. Optical coherence tomography reveals distinct patterns of retinal damage in neuromyelitis optica and multiple sclerosis. PLoS One 8 (6), 1–10.
Siffrin, V., Vogt, J., Radbruch, H., et al., 2010. Multiple sclerosis–candidate mechanisms underlying CNS atrophy. Trends Neurosci. 33 (4), 202–210.
Siger, M., Dzięgielewski, K., Jasek, L., et al., 2008. Optical coherence tomography in multiple sclerosis. J. Neurol. 255 (10), 1555–1560.
Smith, S.M., 2002. Fast robust automated brain extraction. Hum. Brain Mapp. 17 (3), 143–155.
Smith, S., Jenkinson, M., Woolrich, M., et al., 2004. Advances in functional and structural MR image analysis and implementation as FSL. NeuroImage 23, S208–S219.
Syc, S.B., Saidha, S., Newsome, S.D., et al., 2012. Optical coherence tomography segmentation reveals ganglion cell layer pathology after optic neuritis. Brain 135, 521–533.
Tam, R.C., Traboulsee, A., Riddehough, A., et al., 2011. The impact of intensity variations in T1-hypointense lesions on clinical correlations in multiple sclerosis. MSJ 17 (8), 949–957.
Toosy, A., Mason, D., Miller, D., 2014. Optic neuritis. Lancet Neurol. 13 (1), 83–99.
Trip, S., Schlottmann, P., Jones, S., et al., 2005. Retinal nerve fiber layer axonal loss and visual dysfunction in optic neuritis. Ann. Neurol. 58 (3), 383–391.
Walter, S.D., Ishikawa, H., Galetta, K.M., et al., 2012. Ganglion cell loss in relation to visual disability in multiple sclerosis. Ophthalmology 119 (6), 1250–1257.
Whittall, K., MacKay, A., 1969. Quantitative interpretation of NMR relaxation data. J. Magn. Reson. 84 (1), 134–152 1989.
Wingerchuk, D., Bandwell, B., Bennett, J., et al., 2015. International consensus diagnostic criteria for neuromyelitis optica spectrum disorders. Neurology 85, 177–189.
Yu, C., Lin, F., Li, K., et al., 2008. Pathogenesis of normal-appearing white matter damage in neuromyelitis optica: diffusion-tensor MR imaging. Radiology 246 (1), 222–228.
Zimmermann, H., Freing, A., Kaufhold, F., et al., 2012. Optic neuritis interferes with optical coherence tomography and magnetic resonance imaging correlations. Mult Scler J 19 (4), 443–450.